A&A manuscript no.
(will be inserted by hand later)

Your thesaurus codes are:
04 (04.19.1) 13 (13.09.1; 13.09.3)

ASTRONOMY
AND
ASTROPHYSICS
11.10.1996

First data from the ISOPHOT FIR Serendipity Survey*

S. Bogun[1], D. Lemke[1], U. Klaas[1,2], U. Herbstmeier[1], R. Assendorp[3], G. Richter[3], R. Laureijs[2], M. F. Kessler[2], M. Burgdorf[2], B. Schulz[2], G. Pelz[1,2], C. A. Beichman[4], and M. Rowan–Robinson[5]

[1] Max–Planck–Institut für Astronomie, Königstuhl 17, D–69117 Heidelberg, Germany
[2] ISO Science Operations Centre, Astrophysics Division of ESA, Villafranca, P.O. Box 50727, 28080 Madrid, Spain
[3] Astrophysikalisches Institut Potsdam, An der Sternwarte 16, D–14482 Potsdam, Germany
[4] Infrared Processing and Analysis Center, JPL, California Institute of Technology, MS 100/22, Pasadena, CA 91125, USA
[5] Imperial College of Science, Technology and Medicine, The Blackett Laboratory, Prince Consort Road, London SW7 2BZ, United Kingdom

Received ¡date¿; accepted ¡date¿

Abstract. The ISOPHOT Serendipity Survey fills the otherwise unused slew time between ISO's fine pointings with measurements in an unexplored wavelength regime near 200 μm. First results of the Serendipity Survey demonstrate its capabilities in the detection of extragalactic point sources as well as in investigations of the galactic infrared cirrus. With the detection limit for point sources of $\sim$ 1 Jy more than 3000 galaxies will be observed.

Key words: Surveys – Infrared: galaxies – Infrared: ISM: continuum

1. Introduction

The Infrared Space Observatory mostly operates in the pointed mode. In order to increase the overall efficiency of the ISO mission it was decided early during the development phase to use the "dead" time while the satellite is slewing from one target to the next for scanning the sky with the ISOPHOT C200 camera (Lemke & Burgdorf 1992).

Since the locations of the slews are determined by the sequencing of the pointings done by the mission planning software, and furthermore the shape of the individual slew is unpredictable, the survey is called ISOPHOT far–infrared Serendipity Survey.

During the "Performance Verification Phase" (PV, Kessler et al. 1996) the Serendipity Survey mode was successfully tested by performing a number of dedicated slew measurements. On January 23, 1996 the routine Serendipity Survey started. So far (until ISO revolution 229 on July 3) around 2000 slew measurements have been performed, adding up to a total slew length of some 36 000°. The distribution of slew lengths is shown in fig. 1a. The covered area is $\sim 1700\Box^\circ$. Approximately 15% of the sky will be covered during the entire ISO mission; about 2% of the sky will be covered two or more times. One region containing the north ecliptic pole and located at $70^\circ < l < 110^\circ$ and $10^\circ < b < 60^\circ$ is visible throughout the mission. Approximately 19% of this region has already been observed. By the end of the mission more than 60% of this area will be covered; 20% of it twice or more. Table 1 summarizes some characteristics of the survey.

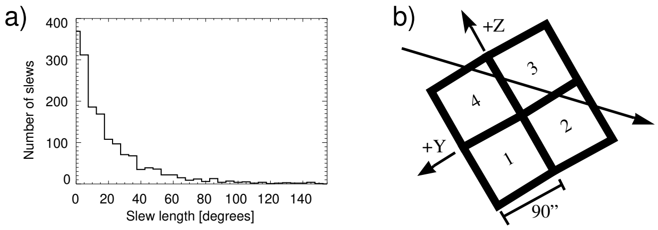

Fig. 1. a) Histogram of the slew length distribution until rev. 229. The binsize is 5°. **b)** C200 pixels in the satellite's coordinate system. The arrow illustrates a point source crossing the array during a slew.

2. Technical performance

The survey is performed with ISOPHOT's C200 array camera using the broad–band filter centered at 175 μm with $\Delta\lambda = 90\,\mu$m (Klaas et al. 1994). Each of the four detector pixels of the camera covers an area of $89.4'' \times 89.4''$ on the sky. The read–out settings are fixed for all slews to $1/8$ s integration time and 3 non-destructive readouts per integration cycle. These values are selected to cope with the maximum slew speed and to match the dynamic range to the variety of expected sky sur-

Send offprint requests to: S. Bogun (bogun@mpia-hd.mpg.de)

* Based on observations with ISO, an ESA project with instruments funded by ESA Member States (especially the PI countries: France, Germany, the Netherlands and the United Kingdom) and with the participation of ISAS and NASA.

Table 1. Characteristics of the ISOPHOT Serendipity Survey.

Detector C200	Pixel size	Filter peak wavelength	Filter width	Airy disk diameter	Integration cycle	Maximum slew speed	Positional accuracy	Point source detection limit	Expected total slew length	Total sky coverage
2x2 pixels	$89.4'' \times 89.4''$	175 μm	90 μm	$2.2'$	1/8 s	$8'$/s	$1'$	$\sim$ 1 Jy	125 000°	$\sim 15\%$

face brightness in the most optimal way. For details of the ISOPHOT instrument see Lemke et al. (1996).

The slew measurements are scheduled automatically by the Mission Planning software. The minimum duration of a slew to activate the Serendipity command sequence is 30 s. If the available slew time exceeds $\sim$ 75 s, a 16 s measurement with one of the internal calibration sources (FCS) is performed at the beginning of the slew in order to monitor the actual calibration of the four C200 pixels.

The slew speed of the ISO satellite reaches a maximum of $\sim 8'/\mathrm{s}$ after a phase of nearly constant acceleration. At the end of the slew, it decelerates with a nearly constant rate. Both acceleration and deceleration are of the order 7 – $15''/\mathrm{s}^2$. Therefore, the data processing has to cope with variable slew speeds which produce varying signal widths for celestial sources.

The raw data generated from the spacecraft and instrument telemetry are processed using the ISOPHOT Interactive Analysis[1] package supplemented by dedicated routines. For each slew a data product containing surface brightness against sky position is computed. These C200 slew profiles are compared with IRAS road maps generated from the ISSA plates (Wheelock et al. 1994).

Next, an algorithm to extract point sources (hereafter called *"PSE"*) is applied to the data: For each position along a given slew PSE derives a gradient vector of the spatial brightness distribution given by the four pixels. The gradients are smoothed by an adaptive filter to enhance their signal–to–noise ratio. When a source is crossed, the vector should point to the peak of the source profile. The intersection of all vectors pointing to the same source should mark its position. In reality, the intersection points scatter around the true source position within a few arcmin. Source candidates are characterized by a cluster of intersection points. Verification of these candidates is done by fitting a two–dimensional Gaussian to the surface brightness data, thereby confirming the point–like character of the target. The fit delivers source position and flux density. A more thorough description of PSE will be given elsewhere (Assendorp et. al, in prep.).

The results presented here are derived using a preliminary version of PSE, therefore the positional and flux uncertainties are somewhat larger (by $\sim 1'$ and $\sim$ 20%, respectively). Point sources down to signal–to–noise ratios (SNR) of $\sim$ 3 can be detected. The limiting SNR, however, can differ from slew to slew and has to be investigated based on a larger sample of detections. For the detected sources (cf. Sect. 3) SNR= 3 corresponds to flux densities of $\sim$ 1 Jy. For all sources outside the galactic plane the detection limit is given by the detector noise, where Franceschini et al. (1991) estimate an average confusion limit (5σ) of $\sim$ 50 mJy.

The uncertainty of the absolute intensities is estimated to be $\sim$ 40%. This value is dominated by the current calibration uncertainties. Signal drifts along the slew and responsivity variations caused by high energy particles also contribute to this value. The calibration stability along a slew, however, is much better.

3. Galaxy detections

The bulk of discrete point sources expected to be brighter than 1 Jy at 175 μm are galaxies (e.g. Bogun 1995). We expect to detect up to $\sim$ 3000 galaxies assuming a sensitivity limit of 1 Jy and a sky coverage of 15% (see also Pearson & Rowan–Robinson 1996). Table 2 presents nine sources seen along slews at high galactic latitude. All of them have an association with an entry in the IRAS Point Source Catalog (IRAS PSC 1988) and are contained in the NASA Extragalactic Data Base[2] (NED, Helou et al. 1991); the first six sources are members of the Coma galaxy cluster. Figure 2 shows the surface brightness along the slew paths for 4 selected sources and their derived FIR spectra. The occurence of maxima of different intensities at different times for the 4 pixels can be explained by the scanning of the point source during the slew (see fig. 1b).

A colour temperature was derived from the colour–corrected IRAS 60 and 100 μm flux densities assuming a modified blackbody spectrum with an emissivity $\propto \nu^1$. The results are listed in Table 2 together with the 175 μm flux density values, $f_{\mathrm{e},175}$, extrapolated using these colour temperatures. For all galaxies, the observed flux density values are larger than the expected ones. We cannot exclude currently that this is due to a systematic calibration offset. In the near future a larger statistical sample and an improved photometry will be available to decide on the presence of excesses in the very far infrared.

[1] The ISOPHOT Interactive Analysis (PIA) is a joint development by the ESA Astrophysics Division and the ISOPHOT consortium led by the Max–Planck–Institut für Astronomie, Heidelberg.

[2] The derived positions show offsets of a few arcmin with respect to the NED positions. At this time, the ISO positions are derived from preliminary pointing data using a point source extraction algorithm, which is not yet optimised. Considerable improvements in the position reconstruction are expected as knowledge of the satellite and the software evolve.

Table 2. Point sources extracted from Serendipity slews. Given are slew measurement number, name and position of the detected object, signal–to–noise ratios of the source detection in the four C200 pixels, IRAS 60 and 100 μm flux densities, 175 μm flux densities derived, colour temperature of a modified blackbody (emissivity $\propto \nu$) fitted to the 60 and 100 μm flux densities and the 175 μm flux density $f_{\mathrm{e},175}$ extrapolated based on this colour temperature.

Meas. Number	Name	α (J2000)	δ (J2000)	S/N Pix 1	S/N Pix 2	S/N Pix 3	S/N Pix 4	f_{60} [Jy]	f_{100} [Jy]	f_{175} [Jy]	$T_{60/100}$ [K]	$f_{\mathrm{e},175}$ [Jy]
033023	PSC 13100+2848	$13^{\mathrm{h}}12^{\mathrm{m}}25^{\mathrm{s}}.9$	$+28^\circ32'16^{\mathrm{s}}$	<2	<2	5.7	2.5	1.4	2.0	1.8	42	1.1
033025	NGC 5056	$13^{\mathrm{h}}16^{\mathrm{m}}12^{\mathrm{s}}.4$	$+30^\circ57'01^{\mathrm{s}}$	11.1	12.3	<2	<2	1.2	2.8	5.6	34	2.2
033025	PSC 13133+3051	$13^{\mathrm{h}}15^{\mathrm{m}}40^{\mathrm{s}}.3$	$+30^\circ35'20^{\mathrm{s}}$	5.8	3.7	<2	<2	0.7	1.3	2.8	38	0.9
033027	NGC 4911	$13^{\mathrm{h}}00^{\mathrm{m}}56^{\mathrm{s}}.1$	$+27^\circ47'26^{\mathrm{s}}$	7.5	<2	8.9	7.8	0.7	2.5	4.4	29	2.3
033029	NGC 4911	$13^{\mathrm{h}}00^{\mathrm{m}}56^{\mathrm{s}}.1$	$+27^\circ47'26^{\mathrm{s}}$	7.0	12.9	3.8	<2	0.7	2.5	5.5	29	2.3
033029	PSC 13127+3040	$13^{\mathrm{h}}15^{\mathrm{m}}08^{\mathrm{s}}.2$	$+30^\circ24'14^{\mathrm{s}}$	2.4	3.7	3.8	<2	1.0	1.7	2.4	39	1.0
081802	NGC 5156	$13^{\mathrm{h}}28^{\mathrm{m}}44^{\mathrm{s}}.1$	$-48^\circ55'01^{\mathrm{s}}$	23.7	21.7	20.1	2.7	4.1	11.6	14.7	32	9.2
081802	NGC 5266A	$13^{\mathrm{h}}40^{\mathrm{m}}37^{\mathrm{s}}.1$	$-48^\circ20'34^{\mathrm{s}}$	14.1	6.0	19.2	10.2	1.8	5.7	6.7	30	5.2
082817	NGC 5610	$14^{\mathrm{h}}24^{\mathrm{m}}23^{\mathrm{s}}.1$	$+24^\circ36'50^{\mathrm{s}}$	23.2	4.0	3.8	24.8	4.8	8.7	10.9	38	5.5

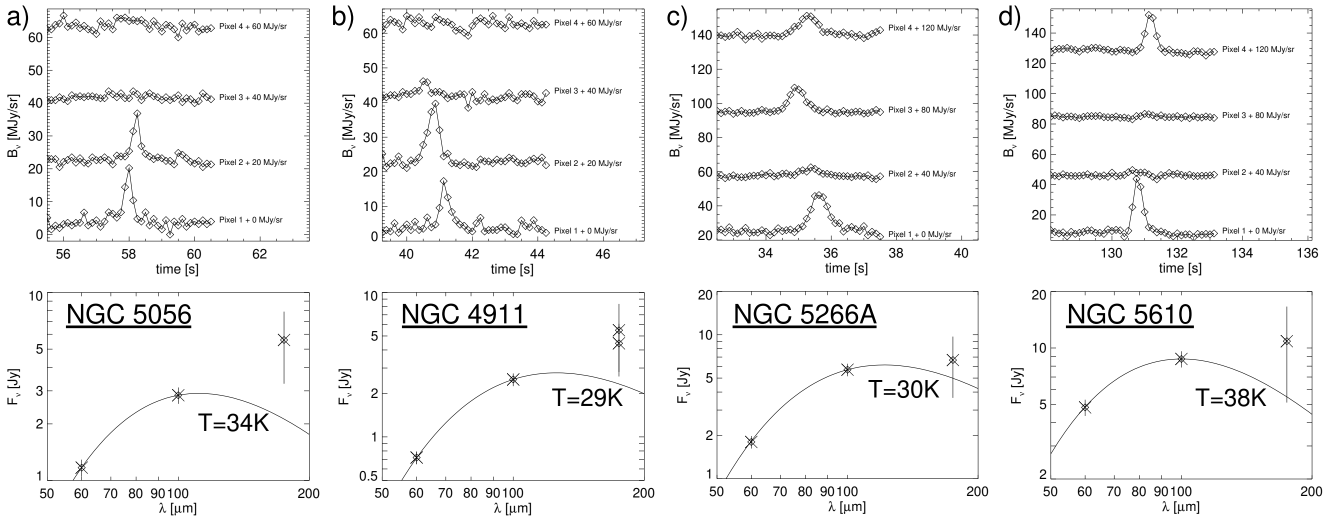

Fig. 2. Surface brightnesses observed in the C200 pixels and FIR spectra for 4 identified sources. Errors comprise the effects described in Sect. 2. The 60 and 100 μm flux densities are taken from the IRAS PSC. For NGC 4911 the flux densities of two detections on different slews are plotted. The solid lines show a modified blackbody spectrum (emissivity $\propto \nu$) fitted to the IRAS 60 and 100 μm flux densities.

4. Observation of the Ursa Major cirrus complex

As an example for Serendipity Mode observations of the galactic cirrus we present a 56.3° long slew crossing the prominent features in Ursa Major (de Vries et al. 1987). They consist of molecular clouds (MBM 23, MBM 22) and atomic hydrogen clouds (ACl 1, ACl 2). In fig. 3a the last 17.3° of the slew are overlayed on the IRAS $100\,\mu$m image. The $175\,\mu$m surface brightness along the slew averaged from the four pixels' intensities is shown in fig. 3b together with the corresponding $100\,\mu$m scan (I_{100}) of the IRAS survey. All clouds with $I_{100} > 1\,\mathrm{MJy\,sr^{-1}}$ are detected at $175\,\mu$m. Peaks at $100\,\mu$m are very closely correlated with peaks in the Serendipity slew. There is a systematic positional offset, which decreases with decreasing slew velocity, an artefact of the preliminary pointing information (cf. footnote 2).

To illustrate variations of the colour ratios along the slew we use a method similar to that of Laureijs et al. (1991). This analysis does not rely on the absolute calibration. The IRAS 60 and $100\,\mu$m and ISOPHOT data were smoothed to the same resolution ($\sim 3'$). Contributions of the zodiacal light and the diffuse galactic emission, derived at slew position 49.5° (as indicated in fig. 3b) were subtracted for all three data sets. For a compact cloud (at slew position 55.15°, labeled "REF"), where the positions of the Serendipity data are reliable, we derived the I_{175}/I_{100} and I_{175}/I_{60} ratios. The IRAS data were then scaled with these computed values and plotted for selected regions in fig. 3c and d. The three curves should coincide if there were no variations of the ratio as compared to the reference cloud.

The close correspondence between the 175 and scaled $100\,\mu$m data shows that the $175\,\mu$m emission arises in the same

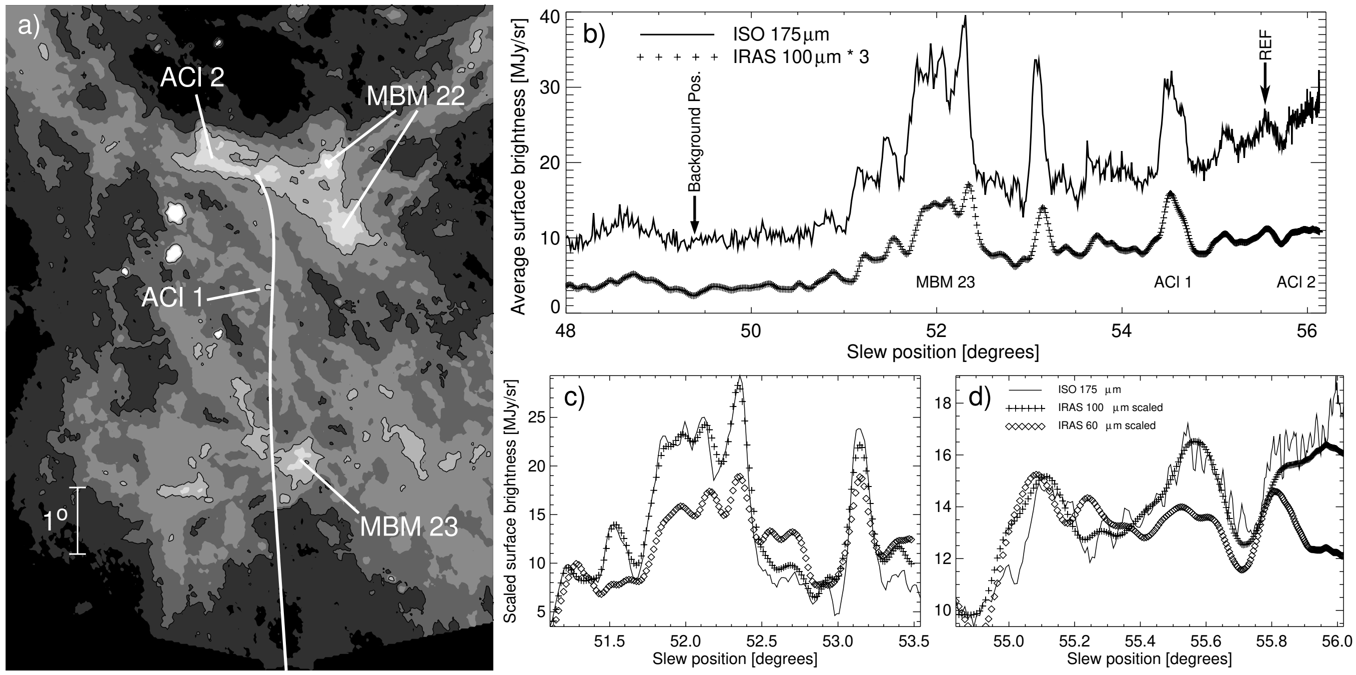

Fig. 3. a) Serendipity slew path overlayed on the 100 μm ISSA image. **b)** Surface brightness along the slew averaged from the four pixels' values: ISOPHOT 175 μm (line), IRAS 100 μm (crosses; scaled with a factor of 3). **c,d)** Scaled surface brightness for two regions: 175 μm (line), 100 μm (crosses), 60 μm (diamonds).

structures as I_{100}. The intensity ratios, however, are not constant along the slew. E.g., the clouds at 55.15° and 55.55° show almost identical 175 and scaled 100 μm ($I_{s,100}$) intensities, whereas I_{175} and $I_{s,60}$ differ significantly only for the cloud at 55.55°. Also in most parts of MBM23, as well as in ACl2 at the end of the slew, I_{175} almost equals $I_{s,100}$. $I_{s,60}$, however, is lower in the cores and higher or equal in the clouds' halos (e.g. at 52.6°). In standard models of the dust FIR emission (e.g. Désert et al. 1990), the I_{175}/I_{100} ratio is dominated by the temperature of the large grains. At 60 μm the emission from transiently heated smaller grains contributes. Colour ratio variations along slews will therefore add information on cloud heating and dust composition.

5. Conclusions

The ISOPHOT Serendipity Survey will complement the pointed observations to increase the efficiency of the observatory. The point source detection limit of $\sim$ 1 Jy will lead to a catalogue containing several thousand sources. This will allow analyses of a large statistical sample of galaxies. The surface brightness detection limit of $\sim 1\,\mathrm{MJy\,sr^{-1}}$ will enable detailed studies of the different components of the interstellar medium, ranging from the cold cirrus to bright reflection nebulae and H II regions. At the end of the mission about 125 000° of slew length will extend the information on the FIR sky at arcmin spatial resolution.

References

Bogun S., 1995, Dissertation, Universität Heidelberg
de Vries H.W., Heithausen A., Thaddeus P., 1987, ApJ 319, 723
Désert F.X., Boulanger F., Puget J.L., 1990, A&A 237, 215
Franceschini A., Toffolatti L., Mazzei P., Danese L., De Zotti G., 1991, A&AS 89, 285
Helou G., Madore B.F., Schmitz M., Bicay M.D., Wu X., Bennett J., 1991, in Egret D. & Albrecht M. (eds.), Databases and On-Line Data in Astronomy, Kluwer Dordrecht, p. 89
IRAS PSC, Version 2.0, 1988, Joint IRAS Science Working Group, U.S. Government Printing Office, Washington D.C.
Kessler M.F., et al., 1996, A&A this volume
Klaas U., Krüger H., Heinrichsen I., Heske A., Laureijs R., 1994, ISOPHOT Observer's Manual, Version 3.1
Laureijs R.J., Clark F.O., Prusti T., 1991, ApJ 372, 185
Lemke D., Burgdorf M., 1992, in: Encrenaz T. & Kessler M. (eds.), Infrared Astronomy with ISO, Nova Science Publishers Inc., p. 69
Lemke D., et al., 1996, A&A this volume
Pearson C., Rowan–Robinson M., 1996, MNRAS, accepted
Wheelock S.L., Gautier T.N., Chillemi J., Kester D., McCallon H., et al., 1994, IRAS sky survey atlas: Explanatory supplement

Acknowledgements. The ISOPHOT project was funded by the Deutsche Agentur für Raumfahrtangelegenheiten DARA, the Max–Planck–Gesellschaft, the Danish, British and Spanish Space Agencies and several European and American institutes. We are indebted to R.D. Joseph and C. Telesco who contributed to the foundation and definition of the scientific goals of this survey.

This article was processed by the author using Springer-Verlag LaTeX A&A style file *L-AA* version 3.